JOURNAL OF PROPULSION AND POWER
Vol. 15, No. 2, March–April 1999

Pyrolysis of Paper and Cardboard in Inert and Oxidative Environments

Ashwani K. Gupta* and Patric Müller†
University of Maryland, College Park, Maryland 20742

Data on the thermal destruction behavior of paper and cardboard under controlled conditions are presented. The decomposition behavior was determined using a thermogravimetric analyzer and differential scanning calorimetry. Tests were carried out on paper, cardboard, and cellulose at two different heating rates of 10 and 50°C/min, and surrounding gas environments of argon (for pyrolysis), air, or oxygen (for oxidative pyrolysis). The temperature range for the thermal decomposition behavior was varied from 25 to 1000°C to investigate the entire decomposition spectra. Global decomposition data show that the maximum decomposition shifts to higher temperatures at higher heating rates as a result of the competing effects of heat and mass transfer, product diffusion, and reaction kinetics. The Arrhenius parameters for thermal decomposition were determined using a first-order decomposition reaction of the form: $dm = -k \times m \times dt$. Results showed that the activation energy, heat of pyrolysis, and char yield are strongly dependent on the heating rate. An increase in heating rate results in a decrease in activation energy and an increased char yield. The heating rate dependence of the kinetic parameters is discussed. The decomposition behavior of the materials examined is endothermic, whereas the overall process is exothermic because of the presence of oxygen in the material. In general, parameters such as heat transfer, mass diffusion, product evolution, heating rate, temperature, and the surrounding environment control the decomposition process. The results show significant variation in the thermal decomposition behavior of the samples. Furthermore, marked variation have been found from sample-to-sample. These variations suggest challenges associated with the exact determination of thermal decomposition characteristics of real wastes. Despite these variations, data presented in this paper are useful for design guidelines for solid waste thermal destruction systems.

Nomenclature

A = pre-exponential factor, min^{-1}
C = constant-volume specific heat, J/kg K
c_p = constant-pressure specific heat, J/kg K
E = activation energy, kJ/mole K
H = enthalpy, J
h = heat of pyrolysis, kJ/mole °C
MW = molecular weight, kg/kmole
m = mass, kg
m_i = initial mass, kg
N = number of moles, kmol
P = power/heat flow, W
p = pressure, Pa
$p(x)$ = series expansion approximating the resulting signal
Q = heat, J
R = specific gas constant, J/kg K
R_u = universal gas constant, J/kmol K
T = temperature, K
t = time, s
U = internal energy, J
V = volume, m^3
W = work, J
α = percent conversion, reaction progress
β = heating rate, °C/min
ρ = density, kg/m^3
ϕ = equivalence ratio

Received Dec. 5, 1997; presented as Paper 98-0264 at the AIAA 36th Aerospace Sciences Meeting, Reno, NV, Jan. 12–15, 1998; revision received Nov. 16, 1998; accepted for publication Nov. 16, 1998.

*Professor, The Combustion Laboratory, Department of Mechanical Engineering. Fellow AIAA.

†Graduate Student, The Combustion Laboratory, Department of Mechanical Engineering.

I. Introduction

THE amount of solid waste generated per person continues to grow in almost all developed countries. Additionally, the reductions in landfill sites, and environmental concern about pollutants generated from incineration, has prompted engineers and scientists to develop an advanced thermal destruction system that provides acceptable (minimum) emissions and negligible harm to human life and the environment.[1–10] Municipal solid wastes have an average heating value of 12,793 J/g (5500 Btu/lb).[1,10] This energy can supplement the fuel requirements in furnaces. Alternatively, the waste fuel can be incinerated in an energy recovery thermal destruction waste facility. The selection of an appropriate method of disposal is based on the characteristics of waste. Thermal destruction offers distinct advantages over other methods because it provides maximum volume reduction (in excess of 80% of the original waste, depending on the chemical composition), energy recovery, and by-products that can be used in several ways, such as building material and road bed construction. The by-products are also nonleachable. The volume reduction can be further enhanced by proper separation and removal of the recyclables such as metals, glass, and other inorganic materials from the waste. Special interest on toxic organic pollutants and trace metal emissions from incinerators came after the risk-assessment findings toward human life.[2] Pollutants such as NO_x, SO_2, HCl, CO, CO_2, unburned hydrocarbons, particulates, and emission of dioxins, furans, and volatile metals have received increased attention from many countries.[3] Concern about pollutants produced as by-products from combustion is common to all combustion processes. It is, therefore, a challenge for a combustion engineer to control and optimize the thermal destruction processes that yields reliable thermal destruction of

wastes, provides high performance, and minimizes emission of all pollutants.

Increasing interest in the thermal destruction of wastes requires a comprehensive understanding of how variations in key parameters, such as temperature, heating rate, chemical composition of the material, and the surrounding environment, influence thermal decomposition of waste. The present study examines the thermal decomposition characteristics of paper and cardboard using a thermogravimetric analyzer (TGA) coupled to a differential scanning calorimeter (DSC). The Arrhenius kinetic parameters have been calculated for the two materials as affected by the heating rate and composition of the surrounding gas. Data are compared with cellulose, which represents the organic portion of wastes.

II. Experimental Procedures

The thermal decomposition of paper, cardboard, and cellulose in inert and oxidative environments was measured using TGA and DSC tests. TGA has been extensively used to determine the global kinetic parameters. The Rheometric Scientific STA 1500 TGA system used is capable of making simultaneous DSC and TGA measurements at temperatures up to 1500°C. Aluminum pans of 4 mm diameter were used to examine materials in the TGA system. Experimental conditions are shown in Table 1.

The samples were subjected to two heating rates (10 and 50°C/min), to study the effects of heating rates on thermal decomposition. Four different gas environments (argon, oxygen, air, and argon, with air addition at 600°C) are considered at each heating rate. All of the tests featured a gas flow rate of 5 ml/min. Figures 1 and 2 show samples used in this study. The light-color samples nominally represent paper (Fig. 1), whereas the darker-color samples (Fig. 2) represent cardboard. The hybrid color represents impurities of other material in the paper sample (see Fig. 1 showing some slightly darker-color material).

Table 1 Experimental conditions of cardboard and paper

Sample	Paper	Cardboard
Material diameter, mm	4–6	3–5
Sample weight, mg	8.875–17.671	4.454–9.484
Sample moisture fraction, %	5	5
Surrounding gas environment	Argon, air, oxygen, and argon with air addition at 600°C	
Gas flow rate, ml/min	5	
Temperature range, °C	25–1000	
Heating rates, °C/min	10 and 50	

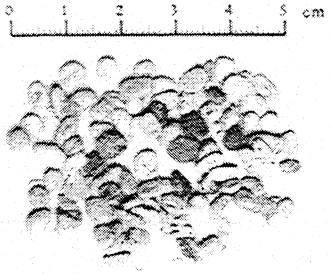

Fig. 1 Photograph of paper sample.

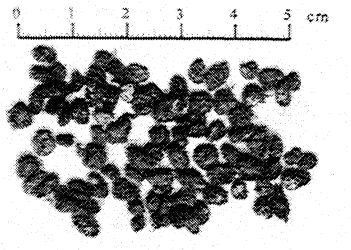

Fig. 2 Photograph of cardboard sample.

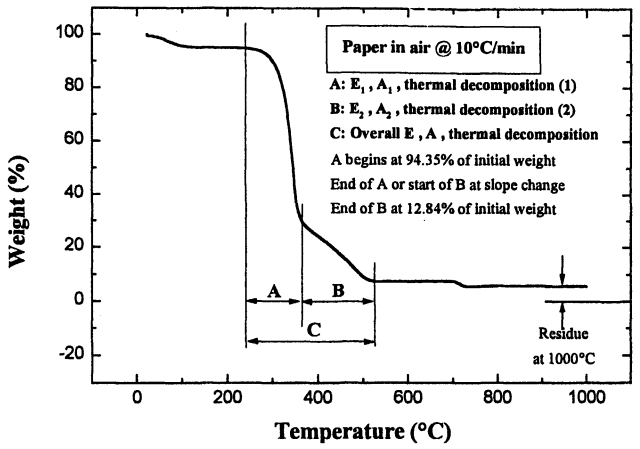

Fig. 3 Definition of E_i, A_i, and thermal decomposition.

Because of differences in the chemical composition of the material, the density of the sampled material varies from sample-to-sample. Important and relevant experimental conditions for the two samples are shown in Table 1.

The mass reduction of the cardboard samples was determined as a function of temperature and time for a given heating rate. The time-dependent information is useful when determining the heat of thermal decomposition as described in the analysis section. The sample weight loss is measured as a function of time, and the calculation of global kinetic parameters is based on simplifying assumptions that may not strictly correspond to the actual chemical reactions that occur during the thermal decomposition process. However, the data provide important information on the reaction parameters such as the temperature and heating rate, and the accompanying effects on material decomposition.

III. Theoretical Analysis

The analysis is carried out by considering different regions of the thermal decomposition process. The procedure allows one to obtain the most useful data during the endothermic and exothermic processes of the waste destruction. A representation of the various destruction stages is shown in Fig. 3. The sample contains ~5% moisture and char (residue).

The Arrhenius parameters E_i and A_i, and the thermal decomposition are defined during the destruction process for characteristic decomposition curves measured in this study. After the initial drying of the material, the first region A starts with the beginning of the thermal decomposition process, which is ~94% of the initial sample weight. The slope change indicates the end of region A, which is also the beginning of region B. Area B ends when there is no further change in the slope. The overall decomposition process is from the beginning of region A to the end of region B, and is indicated as region C.

A. Determination of the Arrhenius Parameters

The Arrhenius parameters for the thermal decomposition of the samples were determined assuming a first-order reaction ($n = 1$).[7] The rate constants are defined as

$$k(T) = A \times \exp\{-[E/(R \times T)]\} \tag{1}$$

Equation (1) defines the temperature dependence of the specific rate constant. A second equation that relates the reaction progress to time through the rate constant is also required:

$$\frac{d\alpha}{dt} = k(T) \times (1 - \alpha)'' \tag{2}$$

Using Eqs. (1) and (2), the initial equation for the McCarty and Green technique can be expressed as:

$$\frac{d\alpha}{dt} = \frac{A}{\beta} \times \exp\left(-\frac{E}{R \times T}\right) \times (1 - \alpha) \quad (3)$$

Rearranging Eq. (3) and integrating yields:

$$-\ell n(1 - \alpha) = [(A \times E)/(\beta \times R)] \times p(x) \quad (4)$$

where $p(x)$ is a series expansion approximating the resulting integral:

$$p(x) \cong \left[\frac{x + 3}{x(x + 1)(x + 4)e^x}\right] \quad (5)$$

Taking the natural logarithm of both sides of Eq. (4) yields:

$$\ell n[-\ell n(1 - \alpha)] = \ell n[(A \times E)/(\beta \times R)] + \ell n[p(x)] \quad (6)$$

Assigning $F(\alpha) = \ell n[-\ell n(1 - \alpha)]$, and subsequently, differentiating with respect to x, yields:

$$\frac{dF(\alpha)}{dx} = \frac{d\ell n[p(x)]}{dx} \quad (7)$$

Substitution for dx, where $dx/d(1/T) = E/R$, yields:

$$E = R \times \frac{dF(\alpha)/dT^{-1}}{d\ell n[p(x)]/dx} \quad (8)$$

The numerator in Eq. (8) is the slope of the plot of $F(\alpha)$ vs $1/T$. The data to construct this plot are taken from the TGA curve. The denominator can be estimated from the series:

$$\frac{d\ell n[p(x)]}{dx} = \frac{1}{x + 3} - \frac{1}{x} - \frac{1}{x + 1} - \frac{1}{x + 4} - 1 \quad (9)$$

The numerator is also a function of E; hence, an initial guess of 30 kcal/mole °C is used for the activation energy. A series of iterative calculations are used to refine the value for E within 0.1 cal. Once E has been determined, the pre-exponential factor A is calculated using Eq. (9).

B. Determination of the Maximal Decomposition Temperature

The thermal decomposition process can be expressed with the curve $m(t)$ or $m(T)$, which is the actual weight vs time or temperature as shown in Fig. 4.

The temperature commensurate with the maximum decomposition rate is the point of maximum slope of this curve. It can be determined by calculating

$$\frac{dm}{m} = \frac{m_i - m_{i-1}}{m_{i-1}} = \frac{m_i}{m_{i-1}} - 1 \quad (10)$$

The point of maximum decomposition can be obtained by plotting dm/m vs time or temperature, and is the minimum of this curve:

$$\left(\frac{dm}{m}\right)_{max} = f(t_{max}) = f(T_{max}) \quad (11)$$

C. Determination of the Heat of Pyrolysis

The caloric equation of state in differential form can be written as

$$dh = \left(\frac{\partial h}{\partial T}\right)_p \times dT + \left(\frac{\partial h}{\partial p}\right)_T \times dp \quad (12)$$

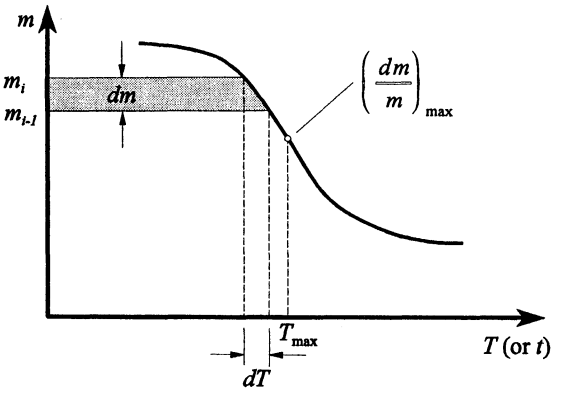

Fig. 4 Determination of the maximum decomposition temperature.

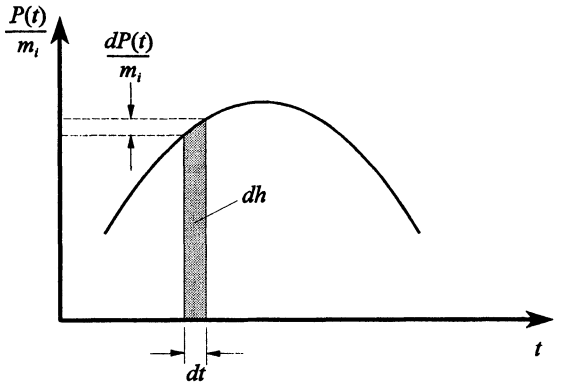

Fig. 5 Determination of the heat of pyrolysis.

The contribution of the second term in (12) is much smaller as compared with the first term (negligible pressure dependence). Equation (12) simplifies to

$$dh = \left(\frac{\partial h}{\partial T}\right)_p \times dT = c_p \times dT \quad (13)$$

Furthermore,

$$dQ = dH = P(t)\, dt = m_i c_p\, dT \quad (14)$$

Dividing both sides of Eq. (14) by the initial sample weight, yields

$$dh = \frac{P(t)}{m_i}\, dt \quad (15)$$

After the integration of Eq. (15) over time, the heat of pyrolysis can be determined as

$$h = \int_{t_1}^{t_2} \frac{P(t)}{m_i}\, dt = \frac{1}{m_i} \times \int_{t_1}^{t_2} P(t)\, dt \quad (16)$$

The heat of pyrolysis is the area under the curve $P(t)/m_i = f(t)$, as shown in Fig. 5. The heat of pyrolysis was determined for regions A, B, and C. This procedure yields information on the thermal decomposition process, which takes into account the various distinct stages that occur during the thermal decomposition process.

IV. Results and Discussion

A. TGA/DSC Results for Cardboard and Paper

Typical results on the pyrolysis in an inert environment, at a heating rate of 50°C/min, are shown in Figs. 6 and 7 for

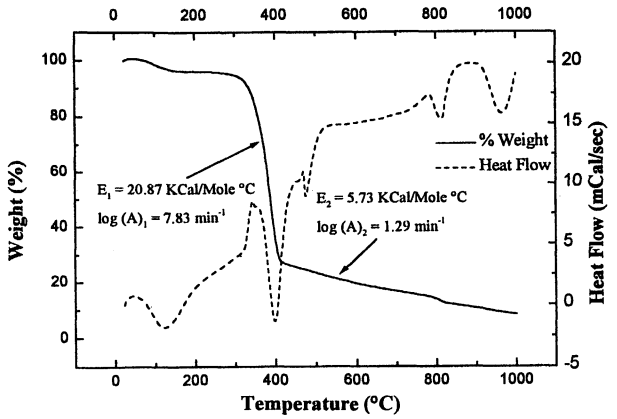

Fig. 6 Thermal decomposition results for paper in an argon environment at 50°C/min.

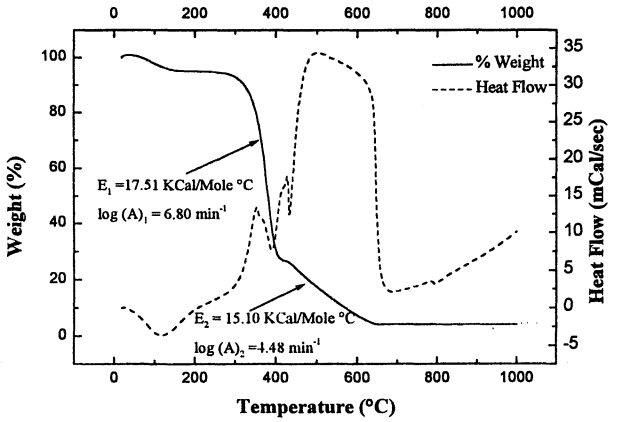

Fig. 7 Thermal decomposition results for cardboard in an argon environment at 50°C/min.

paper and cardboard, respectively. The surrounding gas flow rate was kept at 5 ml/min. The effect of surrounding gas flow rate was found to be negligible. The results show mass evolution (TGA data) and heat flow into or out of the sample (DSC data) as a function of temperature surrounding the material. They also show the presence of residue (char) at the end of the heating period (at 1000°C) in every sample.

Measurements indicate that both samples decomposed in two different stages, except for the drying process at the beginning of the test (up to 110°C). The decomposition was found to shift to higher temperatures at higher heating rates (temperature corresponding to maximum slope in the TGA curve). The char yield at the end of the tests (at a temperature of 1000°C) and the temperature of maximum decomposition depend on the experimental conditions (see Table 2). This arguably suggests that the global decomposition kinetics appear to be heating rate dependent, which remains a controversial issue.[5-10] Heat transfer limitations alone cannot explain the observed shift, and the mass transport limitations can play a major role as heating rate increases.[7,8] It is suggested that tar evaporation is a key aspect of the mass transport process, which, in turn, is a strong function of the heating rate.[7] It is also believed that at longer residence time of tars in the reaction chamber, there will be more cracking, via secondary reactions, which results in a shift from char to volatiles emission.

The trend of the char yield at 1000°C is shown in Fig. 8. It shows that cardboard has less char yield than paper. This can be explained by the larger amounts of inorganic material, e.g., calcium carbonate, $CaCO_3$, in paper than cardboard. Furthermore, the value of char yield increases more in the inert environment than oxidative environment. This is attributed to the oxidation of char material in the oxidative environment. This

Table 2 Residue and maximum decomposition temperature

Surrounding gas environment	Heating rate, °C/min	Residue, %	Maximum decomposition temperature, °C
Paper			
Argon	10	5.66	348
	50	8.3	398
Air	10	5.58	348
	50	6.33	383
Oxygen	10	7.04	383
	50	7.78	393
Argon + air at 600°C	10	6.83	350
	50	7.07	393
Cardboard			
Argon	10	3.3	358
	50	4.18	388
Air	10	5.27	355
	50	5.32	386
Oxygen	10	5.46	374
	50	5.63	442
Argon + air at 600°C	10	4.98	348
	50	5.24	381

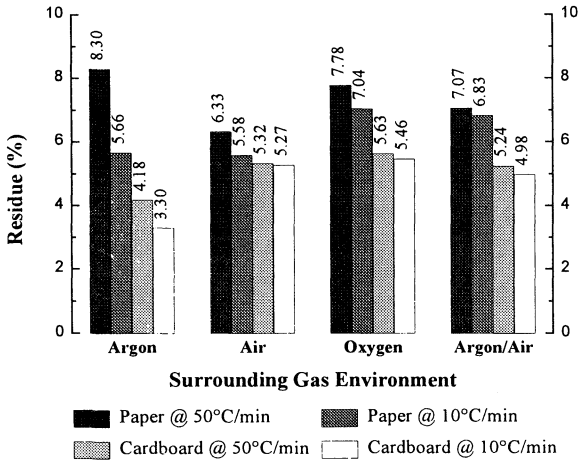

Fig. 8 Residue of paper and cardboard.

is supported by our results that showed that air addition at 600°C (last set of four vertical bars in Fig. 8) yields a reduction in char after air addition.

The calculated Arrhenius parameters (activation energy E and pre-exponential factor A) vs heating rate are shown in Table 3. An increase in heating rate yields a decrease in both activation energy and the pre-exponential factor. It is also important to note that the pre-exponential factors increase with changes of surrounding gases from argon to air. As an example, the value of A for cardboard varies from 16,596 collisions/min in argon to 3,548,134 collisions/min in oxygen (oxidative environment) at a heating rate of 10°C/min. This increase of A can be seen for both samples at all regions, and shows that the molecular collisions per unit time during the thermal destruction process increase in oxygen-rich environments. The differences between cardboard in oxygen and argon for region A suggests that mass transfer must have an effect in addition to the varying sample conditions, such as, the sample chemical composition, variation in surface area, material porosity, and density.

The overall activation energy (E) for the samples are shown in Fig. 9. The results show a decrease in activation energy with an increase in heating rate caused by the changed heat transfer from ambient to the sample and vice versa. The addition of air at 600°C has no effect on the activation energy. The only detected difference between argon and argon with air addition at 600°C is the char yield. Small variations in

Table 3 Arrhenius parameters for paper and cardboard

Surrounding gas environment	Heating rate, °C/min	Sample weight, mg	E_1, kJ/mole °C	log (A_1), min^{-1}	E_2, kJ/mole °C	log (A_2), min^{-1}	E, kJ/mole °C	log (A), min^{-1}
Paper								
Argon	10	8.875	104.08	9.28	75.03	5.24	47.6	3.65
	50	10.541	87.38	7.83	23.99	1.29	25.5	2.15
Air	10	17.671	104.46	9.38	109.74	8.25	53.8	4.3
	50	16.474	84.7	7.72	48.14	3.18	33.2	2.81
Oxygen	10	15.046	89.97	8.2	377.69	31.22	78.8	7.12
	50	8.988	80.68	7.37	32.15	1.95	27.47	2.32
Argon + air at 600°C	10	12.288	103.16	9.2	71.01	4.75	43.04	3.21
	50	9.837	83.23	7.59	26.54	1.46	24.79	2.05
Cardboard								
Argon	10	5.198	56.81	4.88	111.5	8.42	52.92	4.22
	50	9.484	73.31	6.8	63.22	4.48	39.1	3.35
Air	10	5.608	67.87	5.96	162.99	12.87	69.33	5.8
	50	4.454	62.09	5.84	61.71	4.44	37.85	3.25
Oxygen	10	9.242	65.86	5.88	299.78	28.53	72.35	6.55
	50	6.178	89.47	8.59	194.1	15.59	65.77	6.24
Argon + air at 600°C	10	6.808	53.59	4.53	88.63	6.49	50.37	4.15
	50	5.153	45.22	4.28	83.28	6.41	46.47	3.92

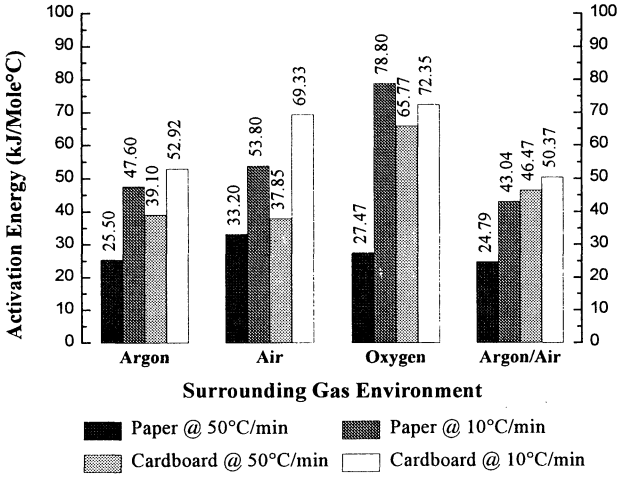

Fig. 9 Overall activation energy for paper and cardboard.

Table 4 Heat of pyrolysis of paper and cardboard

Surrounding gas environment	Heating rate, °C/min	Heat of pyrolysis, kJ/mole °C		
		A	*B*	*C*
Paper	10	963.33	3777.26	4704.59
	50	189.11	2883.16	3072.27
Air	10	466.37	4004.97	4471.34
	50	159.93	2905.46	3065.39
Oxygen	10	681.28	1163.56	1844.84
	50	276.5	3231	3507.5
Argon + air at 600°C	10	904.64	3826.7	4731.35
	50	277.44	3588.7	3866.14
Cardboard				
Argon	10	1712.99	5208.94	6921.92
	50	574.93	3573.85	4148.79
Air	10	1650.76	4059.27	5710.03
	50	1152.09	4978.08	6130.17
Oxygen	10	1058.19	1112.75	2170.94
	50	688.42	1708.51	2396.93
Argon + air at 600°C	10	1283.61	4939.32	6222.93
	50	720.38	4515.49	5235.87

results could be caused by sample-to-sample variations in chemical composition, surface area, and material density.

The activation energy of paper and cardboard decreases with an increase in heating rate, and this is in general agreement with the data reported by Suuberg et al.[6] for cellulose, which can be used as a baseline for the thermal decomposition process of the organic portion of the waste. Data on cellulose have also been obtained, and the results are given in the next section. An examination of the DSC results reveals that the thermal decomposition process of paper and cardboard is exothermic in all of the examined regimes (*A*, *B*, and *C*). The heat of pyrolysis, calculated according to the procedure outlined in Section III.C., for regions A, B, and C are shown in Table 4.

Figure 10 shows that the overall heat of pyrolysis is exothermic for all of the examined conditions. The heat of pyrolysis of cardboard increases with an increase in heating rates in an oxidative environment, and decreases in an inert environment. Paper shows the same trend as cardboard in an inert environment. However, this trend was not observed in the oxidative environment. This may be a result of sample-to-sample variation in the chemical composition. Further insight, therefore, necessitates detailed chemical analysis of the sample.

Results presented here show that thermal decomposition process is equally affected by both heat and mass transfer. The heating rate was found to effect the heat of pyrolysis, activation energy, char yield, and process temperature.

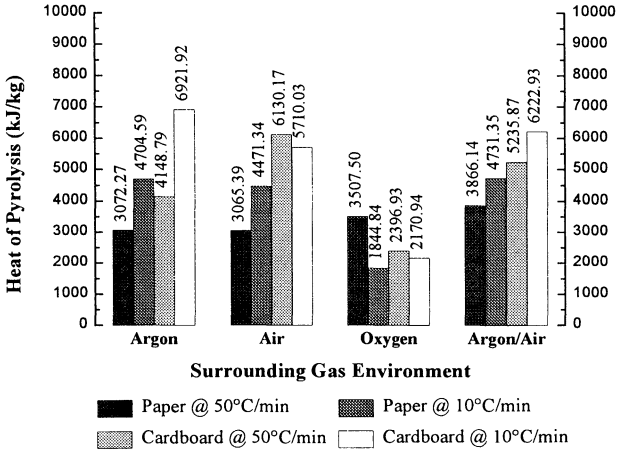

Fig. 10 Overall heat of pyrolysis for paper and cardboard.

B. TGA/DSC Results for Cellulose

Data on cellulose have been obtained to provide a direct comparison with results obtained for paper and cardboard samples. Only two environments of argon and air were considered to show the differences in the thermal decomposition behavior in argon and air environments. The heating rate, temperature

range, and surrounding gas flow rate were the same as that for paper and cardboard samples.

Measurements obtained from TGA and DSC for the cellulose sample at a heating rate of 50°C/min are shown in Fig. 11. Other experimental conditions were the same as that for paper and cardboard. The results show the mass evolution and heat flow into or out of the sample as a function of temperature surrounding the material. Data shown in Table 5 provide a trend on the char yield and temperature of maximum decomposition for cellulose, paper, and cardboard.

The results presented in Fig. 12 show minimum residue for cellulose, and are the highest for paper at both heating rates and surrounding gas environments. The increase in char yield with an increase in heating rate for cellulose is similar to that found for paper and cardboard. At high heating rates, one would expect a higher residence time at high temperatures, which will enhance further cracking of the material. The temperature of maximum decomposition shifts to higher temperatures at higher heating rates.

The Arrhenius parameters vs heating rate are given in Table 6. The overall activation energy of cellulose, including its comparison with paper and cardboard, is shown in Fig. 13. The activation energy of cellulose decreases with an increase in heating rate. These results show the same dependence of A and E as noted for paper and cardboard.

An examination of the DSC results reveals that the overall thermal decomposition process of cellulose is exothermic. Only at high heating rates does region A reveal an endothermic decomposition process. This may be because of limitations of mass and thermal transport at high heating rates. The heats of pyrolysis of cellulose calculated for regions A, B, and C are shown in Table 7. The results are compared with paper and cardboard.

Results on the overall heat of pyrolysis for cellulose, and its comparison with paper and cardboard, are shown in Fig. 14, at two heating rates. They show the trend of a decrease in the heat of pyrolysis with an increase in heating rate. Cellulose shows a decrease in the heat of pyrolysis with an increase in the heating rate. The decomposition behavior of cellulose in an argon and air environment remains essentially unchanged.

The data presented in the preceding text assists in understanding the complex thermal decomposition of real waste ma-

Table 5 Residue and maximum decomposition temperature

Surrounding gas environment	Heating rate, °C/min	Residue, %	Maximum decomposition temperature, °C
Cellulose			
Argon	10	0.68	344
	50	2.14	399
Air	10	0.85	346
	50	3.64	383
Paper			
Argon	10	5.66	348
	50	8.3	398
Air	10	5.58	348
	50	6.33	383
Cardboard			
Argon	10	3.3	358
	50	4.18	388
Air	10	5.27	355
	50	5.32	386

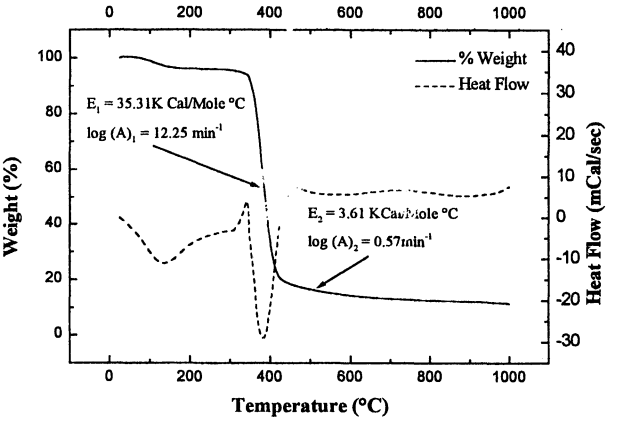

Fig. 11 Thermal decomposition of cellulose in an inert (argon) environment at 50°C/min.

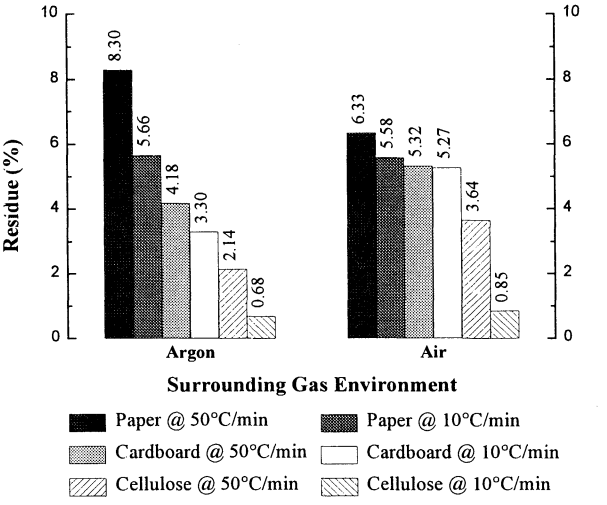

Fig. 12 Residue of all samples.

Table 6 Arrhenius parameters for all samples

Surrounding gas environment	Heating rate, °C/min	Sample weight, mg	E_1, kJ/mole °C	log (A_1), min^{-1}	E_2, kJ/mole °C	log (A_2), min^{-1}	E, kJ/mole °C	log (A), min^{-1}
Cellulose								
Argon	10	20.618	174.42	15.23	32.66	1.33	21.68	1.1
	50	23.889	147.84	12.75	15.11	0.57	11.76	0.47
Air	10	24.998	182.46	16.16	50.41	3.16	38.73	2.72
	50	24.113	154.03	13.29	26.63	1.36	21.05	1.74
Paper								
Argon	10	8.875	104.08	9.28	75.03	5.24	47.6	3.65
	50	10.541	87.38	7.83	23.99	1.29	25.5	2.15
Air	10	17.671	104.46	9.38	109.74	8.25	53.8	4.3
	50	16.474	84.7	7.72	48.14	3.18	33.2	2.81
Cardboard								
Argon	10	5.198	56.81	4.88	111.5	8.42	52.92	4.22
	50	9.484	73.31	6.8	63.22	4.48	39.1	3.35
Air	10	5.608	67.87	5.96	162.99	12.87	69.33	5.8
	50	4.454	62.09	5.84	61.71	4.44	37.85	3.25

Table 7 Heat of pyrolysis for all samples

Surrounding gas environment	Heating rate, °C/min	Heat of pyrolysis, kJ/mole °C		
		A	*B*	*C*
Cellulose				
Argon	10	196.41	3555.92	3752.33
	50	−277.39	2170.35	1892.96
Air	10	197.73	3400.67	3598.4
	50	−156.32	2502.56	2346.25
Paper				
Argon	10	963.33	3777.26	4704.59
	50	189.11	2883.16	3072.27
Air	10	466.37	4004.97	4471.34
	50	159.93	2905.46	3065.39
Cardboard				
Argon	10	1712.99	5208.94	6921.92
	50	574.93	3573.85	4148.79
Air	10	1650.76	4059.27	5710.03
	50	1152.09	4978.08	6130.17

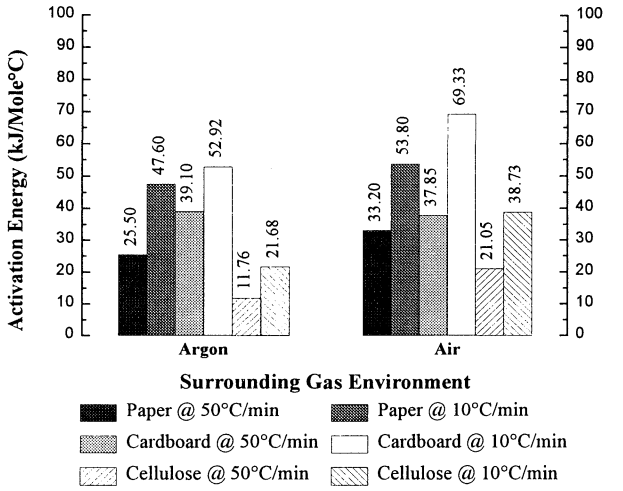

Fig. 13 Overall activation energy for all samples.

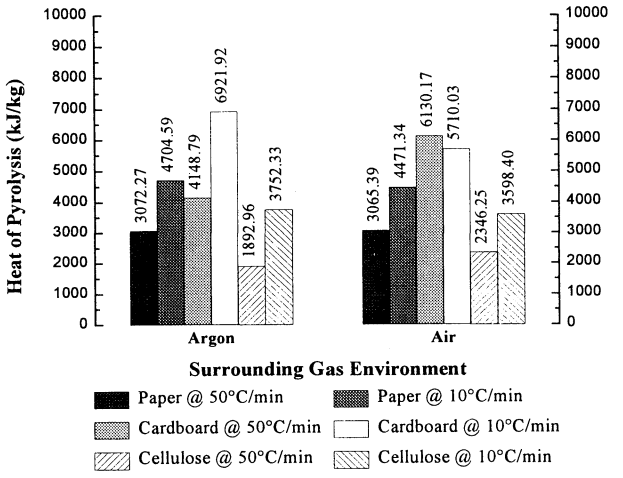

Fig. 14 Overall heat of pyrolysis for all samples.

terials because cellulose represents a major fraction of the organic portion of wastes. Providing an understanding of the thermal decomposition of cellulose helps in determining the basic trends that can then be compared with real waste materials. The following section provides discussion on the differences between the real waste samples of paper and cardboard, and cellulose.

C. Comparison of Results

The results obtained on the waste samples show mainly the same trends. An increase in heating rate generally results in an increase in residue, which can be explained by the longer residence time of the material at high temperatures under lower heating rates. The less char yield of the cellulose samples, compared with that for paper and cardboard, is attributed to the smaller size of the cellulose particles (in the range of 50 −400 μm). Thus, the surface area of the cellulose samples is very large compared with the samples of paper and cardboard.

The temperature at maximum decomposition was generally found to increase with an increase in the heating rate. This temperature was found to be nearly the same for all waste samples in both inert and oxidative environments. This suggests that the surrounding gas environment has a negligible effect on the maximum decomposition temperature. Figure 15 shows the maximum decomposition temperature of cellulose, paper, and cardboard in argon and air environments.

The DSC results for paper, cardboard, and cellulose in argon and air environments show an increase of activation energy with a decrease in heating rate in all three regimes (*A*, *B*, and *C*). Both paper and cardboard samples have a higher activation energy than cellulose. This may be explained by the differences in the surface area of the samples in addition to the differences in chemical composition of the waste samples. Table 6 shows the Arrhenius parameters for all regions, whereas Fig. 13 shows only the overall activation energy. It is remarkable to note that activation energy for cellulose in region A (which represents the most weight loss, about 70–80%), is much higher than paper and cardboard. In contrast, the values in region B are very low, and the overall activation energy is lowest for all of the samples examined in this study. Figure 16

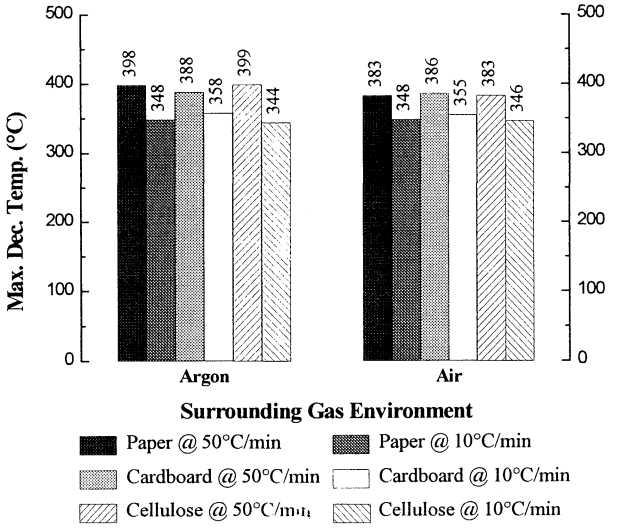

Fig. 15 Maximum decomposition temperature.

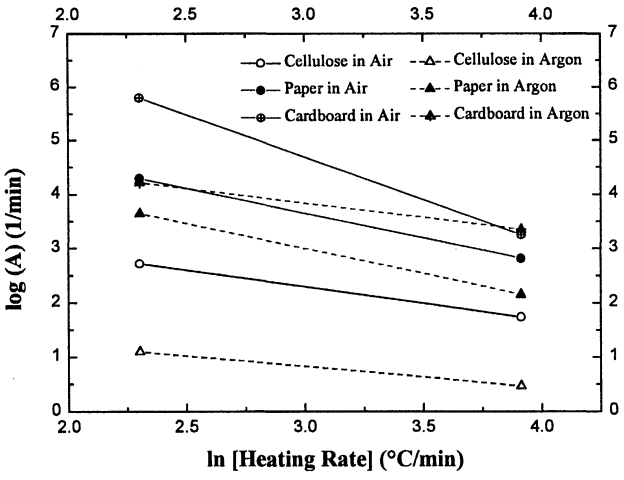

Fig. 16 Pre-exponential factor for all samples in air and argon.

shows the pre-exponential factor A for cellulose and its direct comparison to paper and cardboard. The value of A was found to decrease with an increase in the heating rate. A change of gas from an oxidative to an inert environment decreased the value of A.

The heat of pyrolysis of cellulose is lower compared with the other two samples of paper and cardboard. Cellulose shows the same trend as paper, in which an increase in the overall heat of pyrolysis has been found with a decrease in heating rates. The overall heat of pyrolysis for region C is exothermic for paper, cardboard, and cellulose, as shown by the results shown in Fig. 14 for both argon and air environments. Table 7 shows the same trend for region B. Only region A shows an endothermic reaction at high heating rates for cellulose, whereas paper and cardboard show an exothermic reaction region. This suggests that very high heating rates (associated with heating of the small-size cellulose particles) can decompose particles very rapidly. This also suggests that very high temperatures, such as plasma jet to thermally destruct the waste, can be very instrumental for the thermal destruction of wastes. High heating rates with plasma will enhance the volatiles and reduce char production as a result of further cracking of the residue material.

V. Conclusions

TGA can provide important fundamental information on the thermal destruction characteristics of materials in a controlled environment. The temperature dependence and mass loss characteristics of materials can be obtained from the TGA. This information can be used to obtain Arrhenius kinetic parameters, and therefore, the decomposition rates under defined conditions of pressure, temperature, surrounding gas environment, heating rate, and waste material properties. DSC provides information on the amount of energy needed to thermally destruct solid waste and energy recovered from secondary combustion of solid and gaseous by-products. This information is helpful in characterizing and understanding the thermal decomposition behavior of solid waste materials.

The kinetic parameters have been determined for paper and cardboard. The results have been compared with cellulose. The thermal decomposition of all materials is affected by heating rate, surrounding gas environment, material chemical composition, and temperature. The rate-controlling step (reaction rate) in pyrolysis is dependent on the temperature, composition of the material, and its physical size. An increased heating rate increased the maximum decomposition rate temperature. The results suggest that heat transfer from ambient to particle plays a major role in the decomposition process and is coupled with mass transfer and product evolution during pyrolysis. The product's yield, composition, and their calorific value are highly dependent on the material composition, heating rate, environment in which the process takes place, and ultimate temperature of the material. The use of plasma jet to thermally destruct solid wastes is beneficial for decreasing the amount of residue and physical size of the chamber, and increasing the heating value of the evolved gases. Pyrolysis time was found to be dependent on particle size, material decomposition, and the surrounding gas environment.

Heat transfer and mass transport are equally important in the thermal decomposition process. It was found that the activation energy, heat of pyrolysis, and char yield are strong functions of the heating rate. The heating rate dependency of the decomposition process and the global kinetics is strongly coupled.

Acknowledgments

This work was supported by the Naval Surface Warfare Center, Carderock Division, and is gratefully acknowledged. Technical discussions with Eugene L. Keating and Eugene Nolting are greatly appreciated.

References

[1]Niessen, W. R., *Combustion and Incineration Processes*, Marcel Dekker, New York, 1995.

[2]Wentz, C. A., *Hazardous Waste Management*, McGraw–Hill, New York, 1995.

[3]DeNevers, N., *Air Pollution Control Engineering*, McGraw–Hill, New York, 1995.

[4]Gupta, A. K., "Thermal Destruction of Solid Wastes," *Proceedings of the 2nd International Conference on Energy Conversion and Related Technologies (RAN98)*, Nagoya Univ., Nagoya, Japan, 1998, pp. 108–115.

[5]Antal, M. J., Jr., and Varhegyi, G., "Cellulose Pyrolysis Kinetics: The Current State of Knowledge," *Ind. Eng. Chem. Res.*, Vol. 34, 1995, pp. 703–717.

[6]Suuberg, E., Milosavljevic, I., and Oja, V., "Thermal Effects in Cellulose Pyrolysis: Relationship to Char Formation Processes," *Int. Eng. Chem. Res.*, Vol. 35, 1996, pp. 653–662.

[7]Turns, S. R., *Introduction to Combustion*, McGraw–Hill, New York, 1996.

[8]Missoum, A., Gupta, A. K., Chen, J., and Keating, E. L., "Thermal Behavior Characteristics During the Decomposition of Cellulose and Polystyrene." *Proceedings of the 31st Intersociety Energy Conversion Engineering Conference IECEC-96*, Inst. of Electrical and Electronic Engineers, Piscataway, NJ, 1996, pp. 69–74.

[9]Missoum, A., Gupta, A. K., and Chen, J., "Thermal Destruction of Waste Materials," *Proceedings of the 32nd Intersociety Energy Conversion Engineering Conference, IECEC-97*, Society of Automotive Engineers, Warrendale, PA, 1997.

[10]Gupta, A. K., "Thermal Destruction of Solid Wastes." *Journal of Energy Resources Technology*, Vol. 118, No. 3, 1996, pp. 187–192.